Solar Energy Advances 2 (2022) 100025

Contents lists available at ScienceDirect

Solar Energy Advances

journal homepage: www.elsevier.com/locate/seja

Potential of solar-driven cooling systems in UAE region

Giovanni Brumana*, Giuseppe Franchini, Elisa Ghirardi

Department of Engineering and Applied Sciences, University of Bergamo, Dalmine Italy

ARTICLE INFO

Keywords:
Solar district cooling
5th-generation district
Renewable energy

ABSTRACT

The paper proposes a comparison between three solar-powered plant configurations covering the cooling demand of a residential compound in the UAE region: i) centralized district cooling system, ii) 5th-generation district system and iii) home air conditioning system. A transient numerical model has been developed for each solution. The model includes photovoltaics, battery storage, and electric chillers, and the thermal envelope to evaluate the building cooling loads. An optimization procedure based on particle-swarm algorithms has been implemented with the aim of selecting the best combination of components to achieve a solar fraction of 70% while minimizing budget costs. The simulation results reward solar district cooling with respect to installation costs: -65% compared to domestic air conditioning system and -27% compared to 5th generation district system. Similarly, in terms of energy savings, the centralized district cooling achieves an annual mean COP of 5.92, and the 5th-generation network shows an average annual COP equal to 3.70 whilst the home system reports an average COP equal to 2.83.

1. Introduction

Nowadays, 20% of GHG emissions are attributed to the growing cooling demand of air conditioning [1]. Electric consumption due to cooling systems account for 14% of the peak demand for global electricity use and, specifically, for 65% in the MENA region [2]. With the aim of increasing sustainability, new more efficient and cost-effective strategies must be adopted to reduce emissions with special effort in the field of cooling systems [3].

A suitable way to reduce the environmental impact is to use high-efficient cooling systems. Among them, district cooling (DC) represents the common solution: based on centralized cooling production and chilled water distribution network is able to provide reliable cooling energy with a consistent energy reduction [4] and peak-shaving effect. Furthermore, for projects in new urbanized areas [5,6] the adoption of district cooling improves sustainability of the residential sector, especially if the design is based on detailed modelling and optimization of piping network and cooling plants [7,8]. The recently introduced 5th generation district heating and cooling systems (5GDHC) are a promising option [9] and represent a viable solution for renewable urban thermal energy supply [10]. The new concept shows high performance [11] and capability to integrate a large share of renewable energy compared to traditional district systems [12].

In the last decade, the scientific community focused on improving cooling technologies driven by renewable sources [13,14]. The wide penetration of non-programmable renewable energy sources, such as wind and solar power, creates some problems for grid stability [15]. The utilization of renewables as an energy source for cooling production significantly reduces the consumption of fossil primary energy and allows a better share of renewable energy [16]. Moreover, solar-driven systems benefit from a good superposition between cooling demand and solar irradiance [17]. The most common home solution, based on a vapor compression chiller coupled with photovoltaic modules, represents a very cost-effective system thanks to its ease of integration and market availability [18] even for low-temperature district systems [19]. With the aim of achieving larger cooling production from renewables, the system requires the adoption of an electric energy storage. The electric energy storage represents a crucial aspect of the system's energy balance [20], especially considering the high cost of Li-Ion batteries [21,22].

Unfortunately, the high ambient temperature forces the cooling system to operate under the worst conditions, which has a detrimental impact on performance as well analyzed by Eicker et al. [23]. The most common heat rejection system for residential applications, the dry cooler, shows very low efficiency in hot climates [24,25]. To improve operations and reduce energy consumption, a good solution is to adopt a reliable heat rejection system such as shallow groundwater or seawater (as the average temperature is lower than that of air). In a desertic region such as UAE, the water scarcity limits the use of freshwater, whilst the adoption of brackish water from underground [26] still remains an open possibility.

The complex design of district systems, as reported by Morvaj et al.[27], pushes the scientific community to adopt new analysis meth-

* Corresponding author: Tel.: +39 035 2052348
E-mail address: giovanni.brumana@unibg.it (G. Brumana).

https://doi.org/10.1016/j.seja.2022.100025
Received 30 April 2022; Received in revised form 24 September 2022; Accepted 24 September 2022
Available online 28 September 2022

Nomenclature

A_{PV}	Aperture area of the PV field
$Cap_{battery}$	Battery storage design capacity
Cap_{CC}	Chiller design capacity
$CapEx$	Capital expenditure
CC	Compression chiller
CHW	Cooling water temperature
COP	Coefficient of performance
CRF	Capital recovery factor
$Cost_{PV}$	PV system unit cost
$Cost_{CC}$	Chiller unit cost
$Cost_{battery}$	Battery storage unit cost
DC	district cooling
$E_{chiller}$	Electric energy consumed by the chiller
E_{cost}	Cost of electric energy
EES	Electric energy storage
$E_{impot-export}$	Electric energy grid balance
E_{PV}	Electric energy produced by the PV
f_{min}	Objective function
HX	Heat exchanger
i	Interest rate
$LCOC$	Levelized cost of cooling
$MENA$	Middle East and North Africa
Ny	Component lifespan
OM	Operation and Maintenance costs
Q	Energy load
$Qcool$	Cooling load
SF	Solar fraction
$5GDHC5$	th generation district heating and cooling systems

ods including detailed numerical simulation, as proposed by Wang in [28] or by Oppelt et al. in [29] with the aim of improving the efficiency of the production plant and the network [30]. Furthermore, the use of accurate computer models and simulation tools [31] coupled with optimization procedures [8] is required when the cooling demand is highly variable, as are the energy sources, and requires the implementation of complex management strategy [32].

In the MENA region, the United Arab Emirates propose challenging programs, such as the UAE Energy Plan 2050, to increase the contribution of clean energy to 50 percent and to improve energy efficiency by implementing green energy sources. An annual solar fraction around 70% appears to be an achievable target in terms of energy-savings, compatible with affordable installation costs [33].

Relying on previous research [34,35], this work provides a complete procedure to design an optimized solar district cooling system, from the evaluation of building loads to the sizing of district network, solar devices, and cooling systems.

The model, using the software Trnsys, combines a transient approach with annual simulations of building envelope, distribution network, and energy plant. The optimum sizing of the components is achieved by a multivariable optimization procedure, performed with GenOpt, with the aim of selecting the best solution in terms of energy savings and economic benefits by achieving an annual solar fraction of 70%.

2. Methodology and Building description

The work assesses the modelling and simulation of the whole heating and cooling supply to the user from the renewable power production to the building air conditioning load. The modelling and the simulation are performed in TRNSYS 18 environments: the model, which includes different component libraries, standard or specific, includes a set of mathematical equations to solve the dynamic behavior of the components; a performance map or a physical modeling approach can be used. For the model, special components that are not available in libraries have been modeled in-house. All the input information for the model is detailed in the following paragraphs. At the end of the annual simulation, a list of outputs on different aspects of the system is monitored with different time resolutions (a single time step or an annual basis). The first part of the work assesses the simulation of a real estate residential compound made of 62 single-family houses in the United Arab Emirates. The governmental plan suggests new solutions for energy-efficient new residential districts based on solar-driven technologies. Annual simulations were carried out for Abu Dhabi (UAE). The selected location is representative of the UAE environmental conditions. information on environmental conditions comes from the international Meteonorm database [36] which provides an accurate description of the environment parameters on hourly basis. As shown in Fig. 1, the Abu Dhabi trends report both daily and seasonal remarkable excursions between maximum and minimum temperature coupled with a relevant level of humidity. The air moisture is very high: in the summer period, the relative humidity fluctuates around 80%. This leads to a consistent diffusion of the available solar radiation that affects the solar device efficiency. In Table 1 GHI and DNI of Abu Dhabi are compared with Riyadh condition (Hot and dry climate): on annual basis, they are respectively 2213 kWh/m^2 and 2296 kWh/m^2.

Table 1
Solar irradiance

	Abu Dhabi	Riyadh
Latitude - Longitude	24°28′N 54°22′E	24°38′N 46°43′E
DNI (kWh/m^{2}y)	1605	2269
GHI (kWh/m^{2}y)	1955	2213

The building is a two-floor single-family building of 600 m^2 and a global volume 1725 m^3 that complies with the UAE residential building style. The building geometry and room distribution meet the standard house requirements in the Abu-Dhabi region.

The building load evaluation is based on a detailed model developed in Trnsys 18 [37] coupled with SketchUp software and Trnsys3D plug-in [38]. Combining variations in weather conditions, the numerical model considers, step by step, the shading effects of geometry and radiation on walls and through windows. The model includes temporal and spatial distribution, internal loads due to appliances, lights and occupancy for each room. Gains and load fluctuation have been considered according to the building occupancy and utilization. The envelope elements have been designed according to the Dubai Green-Building Regulation and Specification [39]; a lists of the internal loads and the main building characteristics is reported in Table 2.

Starting from the presented geometry, the architectural model was imported in a Trnsys deck based on the Multizone Building Type to calculate the cooling load over a 1-year period on hourly basis. The cooling demand of the building has been computed according to the procedure proposed in [40] in a transient analysis: a summary of the cooling load is listed in Table 3 and Fig. 2 in terms of sensible and latent cooling load. The cooling load trend shows the daily variations (Fig. 3) due to temperature and irradiance fluctuations while the monthly cooling load highlights the seasonal behavior of the envelope. Tab. 3 reports an annual cooling load of 156717 kWh with a peak load of 47.33 kW. The simulation point out that the latent cooling load accounts for 40% of the annual demand due to the high temperature and humidity levels.

3. Solar cooling systems

The paper presents a deep analysis of three different solar cooling systems for a residential compound: district cooling with a centralized chilled water production plant, 5th generation district system, and home air conditioning system. All procedures proposed in the work have been developed using Trnsys software. The schematics of the plant configu-

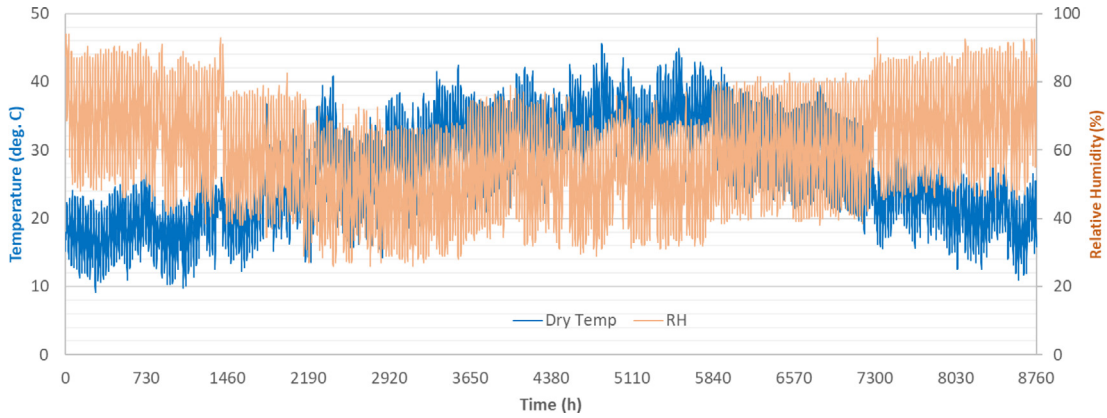

Fig. 1. Ambient temperature and relative humidity

Table 2
Internal loads and comfort specifications

Comfort & Gains			Wall layers & Windows		
Temperature set point	°C	24	Wall thermal transmittance (Uwall)	W/m^2/K	0.57
Relative humidity set point	%	50	Wall thickness	m	0.27
Air changes	Vol/hr	0.60	Wall solar absorptance	%/100	0.30
Recuperative HX efficiency	%	60	Roof thermal transmit	W/m^2/K	0.30
Infiltration	Vol/hr	0.4	Roof thickness	m	0.27
Lighting (peak)	W/m^2	19	Roof solar absorptance	%/100	0.20
Internal gains (peak)	kW	3	Window transmittance	W/m^2/K	1.9
Occupancy (average - max)	Nr.	4 - 10	Solar Energy Transmittance	%/100	0.621

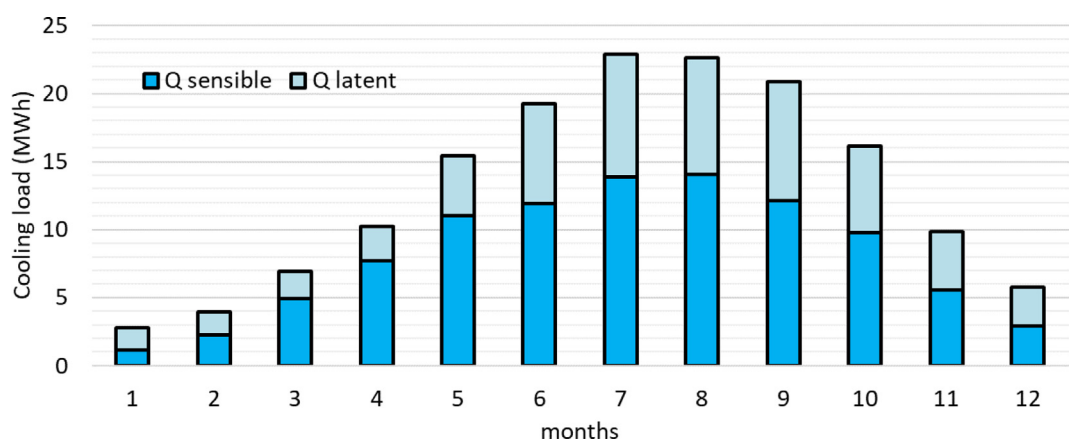

Fig. 2. Building monthly cooling load

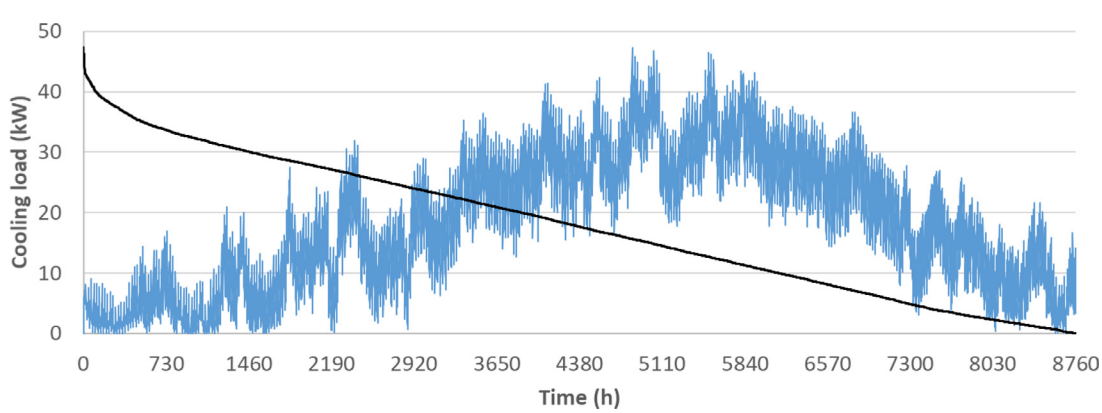

Fig. 3. Cumulated cooling load

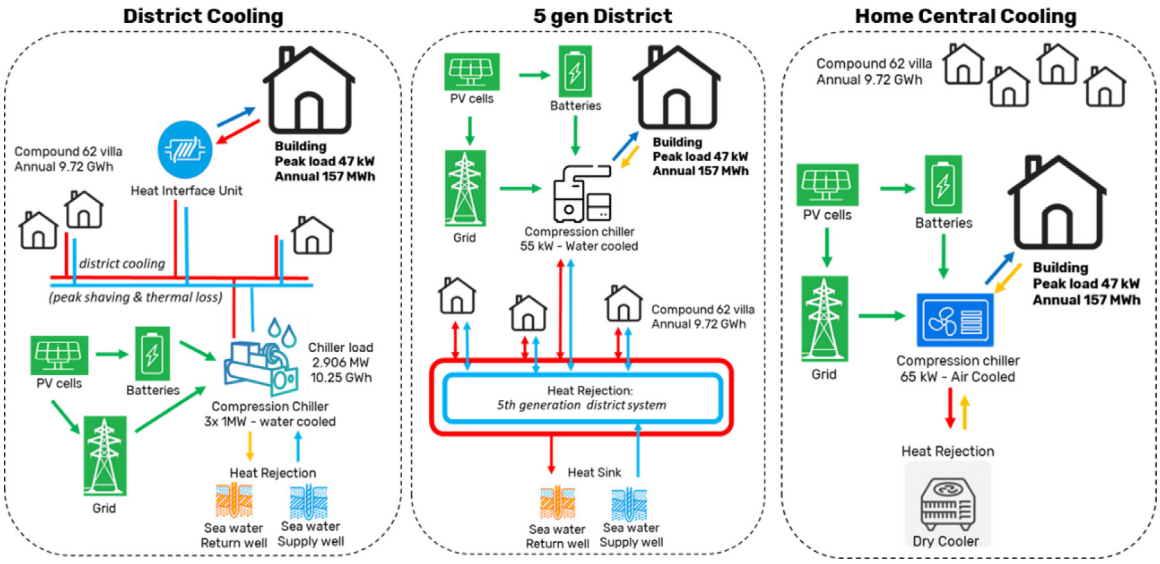

Fig. 4. Solar cooling schematic and specifications

Table 3
Building cooling load

	Peak Load	Annual Load
Sensible cooling load	31.07 kW	97259 kWh
Latent cooling load	18.81 kW	59458 kWh
Global cooling load	47.33 kW	156717 kWh

rations considered are shown in Fig. 4 with some data on building and district cooling load. The cooling loads evaluated in the previous paragraph were adopted as input for the cooling plants. The chiller models are based on market availability, and the performance of the components under design and off-design conditions are evaluated based on the operating maps provided by the manufacturer and according to the heat rejection system.

The systems include a solar field based on a photovoltaic field coupled with Li-Ion batteries. The national power grid is adopted as a backup unit to absorb excess energy, when the batteries have reached maximum capacity, and to supply power to the cooling system, when the renewable energy provided by the PV and batteries is not sufficient to meet the electrical load. The PV modules and batteries specifications are the same for the three layouts and the main parameters are listed in Table 4.

3.1. Centralized district cooling

Starting from the building load, the residential compound cooling requirement was evaluated including the peak shaving effect, the district thermal inertia, and the thermal dissipation through piping. The district system model considers the non-contemporaneity of the cooling load of the individual building and the effect of the piping, as proposed by the authors in [34]. Furthermore, the model includes real conditions such as dynamic thermal losses evaluation and heat transfer substation operation. In order to evaluate the peak shaving effect, the cooling load of each villa is considered equal but, due to the non-simultaneity of the peak loads, the resulting cumulative load is adopted as a normal distribution function. The peak shaving effect reduces the peak cooling load from 2934 kW (47 kW for 62 single houses) to 2755 kW.

The piping network has been designed to meet the demand for compound cooling. The design procedure of the district systems includes a maximum water velocity of 2.75 m/s and 5 cm of piping insulation according to the best practice suggestion [41]. The proposed values represent the characteristics of commercial products [42] and assess the design parameters suggested by the Engineering Association and the pipe manufacturers [43]. To evaluate the heat loss along the network, the temperature difference between the supply line and the return line to the central station is adopted. A user heat transfer substation with a design temperature difference of 7°C ensures cooling delivery, and the control strategy is based on mass flow modulation.

The operation of the district cooling network was simulated coupled with the buildings for a 1-year period. The thermal loss evaluation includes the soil characteristics, the water temperature, and the water velocity. The thermal dispersion increases the required cooling load to the chiller by 5.48% on annual basis (from 9.716 GWh to 10.25 GWh). The central cooling system is based on a water-water industrial chiller and a list of the technical specifications is reported in Table 5. The model is based on the operating maps provided by the manufacturer and presented in Fig. 5 with the aim of evaluating the design and off-design conditions. The rated power is merely an indication of the common components size, the optimum solution adopts the same COP with different sizing. The cooling system is driven by electricity provided from the photovoltaic field coupled with the electric energy storage or by electricity imported from the national grid. The heat rejection system is based on a seawater heat exchanger, where the seasonal water temperature variation is considered to evaluate the chiller performance [44]. The design temperatures of the district system, at the pump station, were selected to be equal to 5 deg. for the supply and 15 deg. C on the return piping.

3.2. 5th generation district heating and cooling

The 5th generation district heating and cooling system represents an innovative solution to provide thermal and cooling energy to the users through a system of cold rings. The district heating and cooling distributes thermal energy at the compound scale in the form of warm and cold flows through a ground-like temperature [10] by reducing thermal dissipation and balancing the energy demand [11] with distributed energy production via reversible water-cooled heat pumps. A similar approach has been considered for the 5th generation district heating and cooling. The pipeline network has been modelled and simulated according to the method proposed in the previous paragraph. Thermal losses were evaluated by considering the instantaneous thermal transmittance between the pipes and the ground.

The 5th generation district heating and cooling is based on two rings, with parallel flows and two levels of design temperatures (18 deg. C for the cold ring and 24 deg. C for the warm one) stabilized by the deep seawater temperature. The operating temperature may vary according to the actual environment condition and the temperature of the supplied

Table 4
Solar fields and battery storage specifications

Solar Field (PV)			Battery storage		
Maximum power (Pmax)	W	250	Total Energy	kWh	14
Module efficiency (ηm)	%	14.91	Usable Energy	kWh	13.5
Temperature coefficient Isc	%/°C	0.051	Apparent Power, max continuous	kVA	5.8
Temperature coefficient Uoc	%/°C	-0.31	Power Factor Range	-	0.85
Temperature coefficient Pmpp	%/°C	-0.41	Round Trip Efficiency	%	90

Table 5
Chiller specifications

	unit	District Cooling value	5 gen District value	Home cooling value
Design chiller capacity	kW	1000*	35*	50*
Design COP	-	5.65 (at 30°C)	3.01(at 35°C)	2.94 (at 35°C)
Design power input	kW	177	11.6	17.0

* The rated power is a mere indication of the common component size and represents the available data.

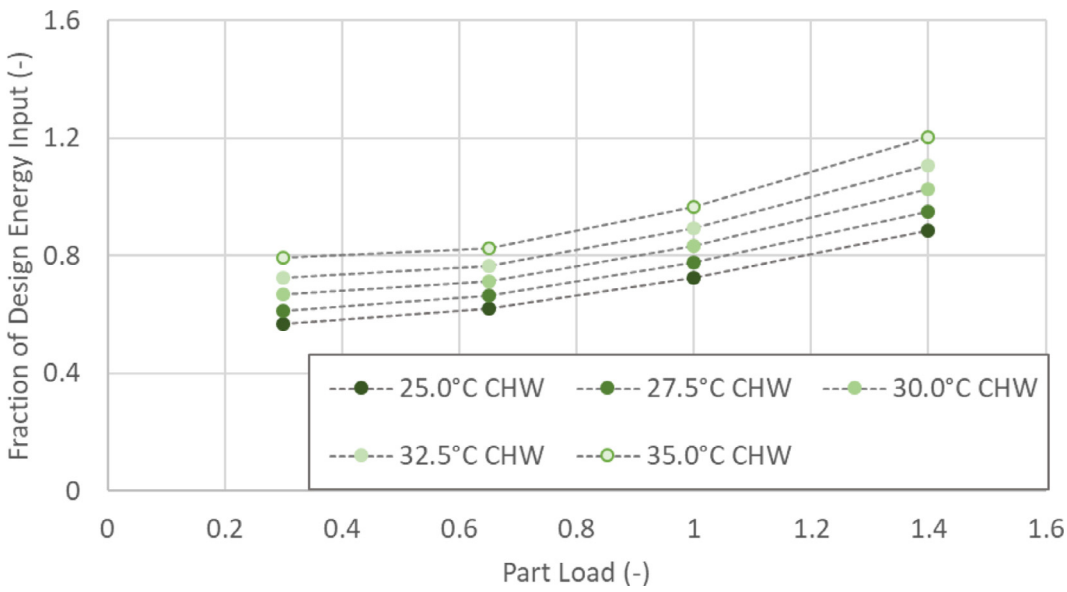

Fig. 5. industrial-grade compression chiller performance maps for centralized cooling plant

seawater. The technical specification were selected according to the best practice suggestions reported in the open literature [12]. In the selected configuration the systems use deep seawater as a heat sink to maintain a constant rings temperature.

The home air conditioning cooling plant coupled with the 5th generation district system is based on a water-water high-efficiency heat pump; the main parameters are reported in Table 5. The performance map provided by the manufacturer (Fig. 6) allows to evaluate design and off-design operation in terms of heat rejection temperatures and part-load derating.

The Fig. 7 shows a comparison between the cumulative cooling load of the district systems. The blue line represents the load of the single building multiplied by 62 while the black and the grey lines show the trend of centralized district cooling systems and 5th generation district respectively. The trends are affected by peak-shaving and thermal losses. The peak shaving effect is the same for both solutions, while for thermal losses the 5th generation district heating and cooling performs better due to the low temperature difference between water flow and soil.

3.3. Home air conditioning

The unit adopted in the home air condition system is based on a high-efficient air-to-water reversible heat pump that meets the demand for cooling and dehumidification. Dry coolers are usually preferred for residential installation and are typically coupled with a compression chiller in water-scarce regions. The heat pump operates in a direct mode without thermal energy storage, and the chiller specifications are listed in Table 4. The adopted unit provide 50 kW of cooling output with a nominal electric consumption of 17 kW. The model includes the dry-cooler component and the instantaneous efficiency has been evaluated based on the performance map provided by the manufacturer. Fig. 8 shows the cooling capacity and coefficient of performance at nominal conditions and at part load conditions for variable ambient temperature levels. The chiller is designed to operate at outdoor temperature up to 50°C, and the cooling capacity was selected to fulfill the peak demand of the building.

4. Optimization

The solar cooling systems have been optimized using GenOpt software, developed by Lawrence Berkeley National Laboratory at University of California, coupled with Trnsys annual simulations. GenOpt is a tool for multivariable optimization of an objective function computed by a simulation program.

The optimization procedure selects a combination of variables (chiller nominal capacity, photovoltaic area, and storage capacity)

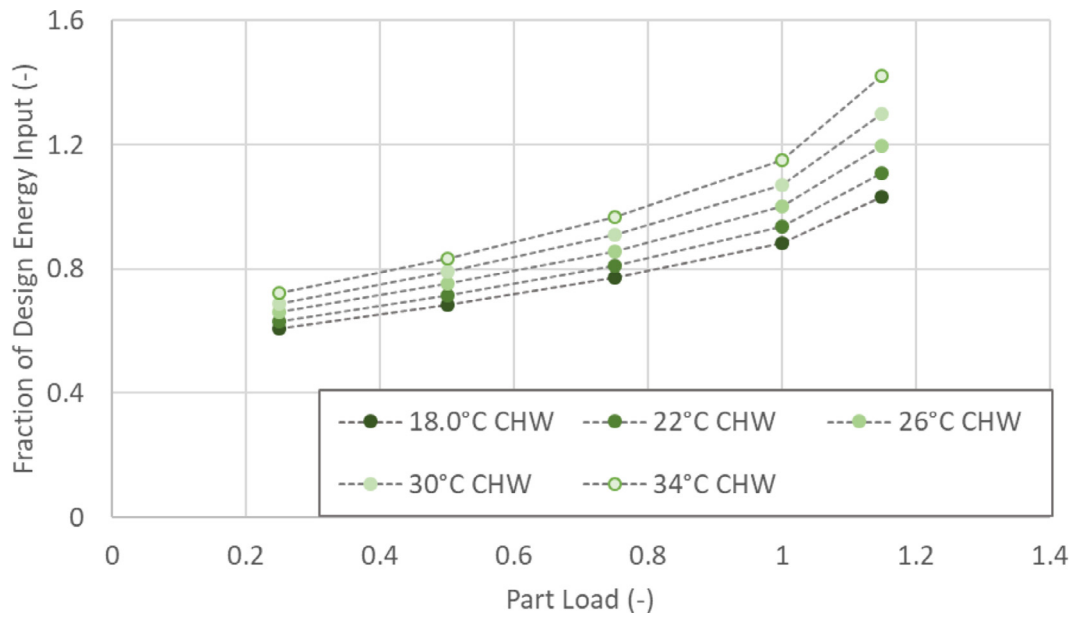

Fig. 6. water-water compression chiller performance maps

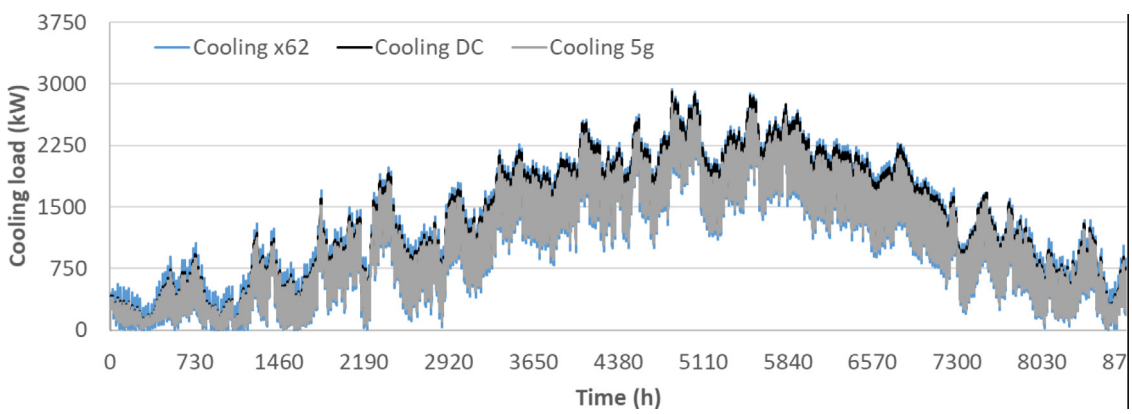

Fig. 7. Cumulated cooling load of district system with respect to single building

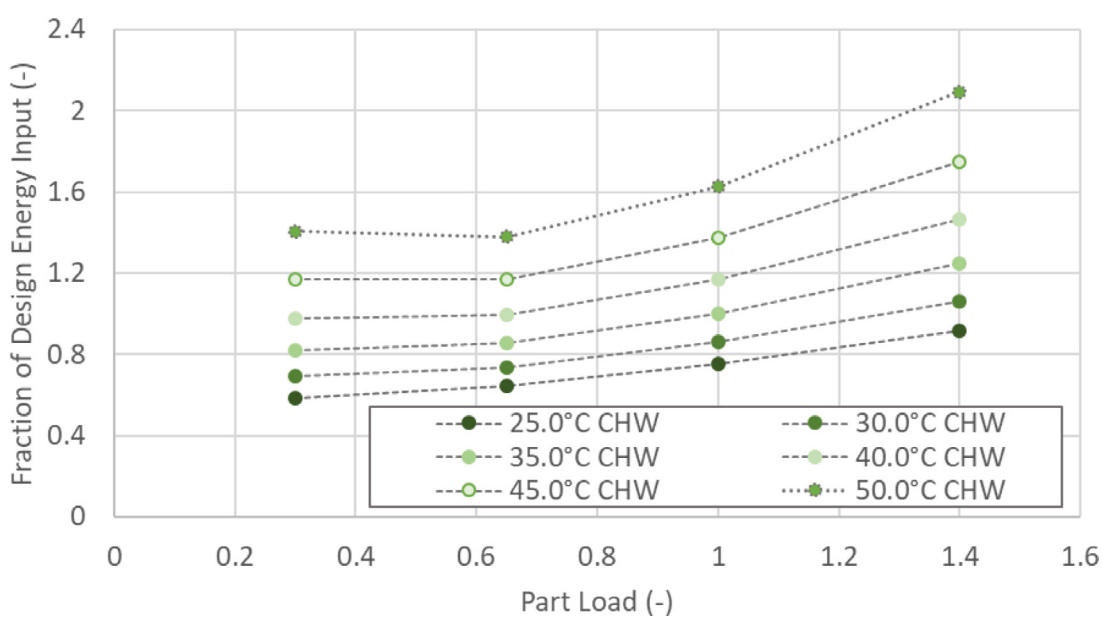

Fig. 8. air-water compression chiller performance maps

Table 6
Optimization variables and related search space

		District Cooling min, max	5 gen District* min, max	Home cooling* min, max
Chiller Rated Capacity	kW	1200, 4000	1200, 5000	2000, 6000
PV field	m^2	4000, 12000	6000, 18000	10000, 22000
Battery	kWh	500, 3000	1000, 4000	1000, 6000

* the reported variables are cumulative (sum of 62 single house)

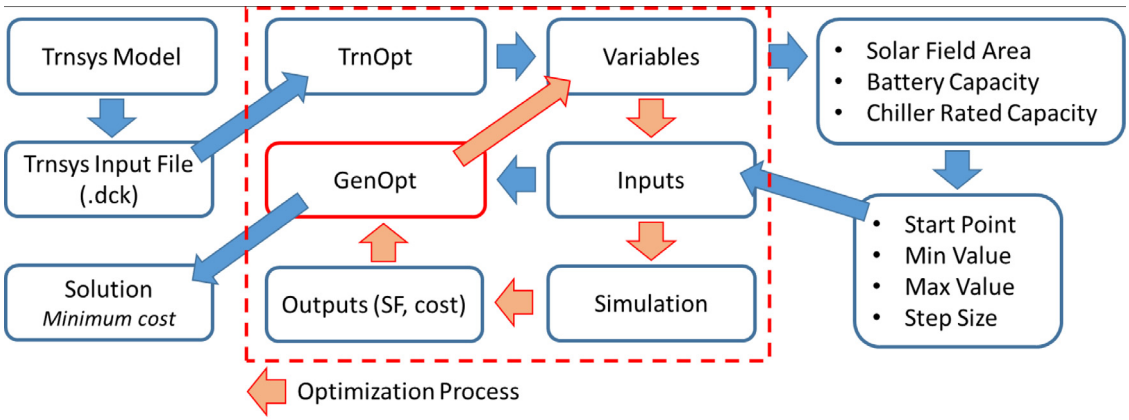

Fig. 9. Simulation and optimization procedure

within the search space, specified in Table 6. The implemented procedure couples two algorithms: the particle swarm and the Hooke and Jeeves, with the aim of improving the global optimum point. The algorithm uses a user-defined number of simulations (seeds and generation for particle swarm) in order to minimize an optimization function [45]. After the first step, the Hooke and Jeeves algorithm identifies the best solution from the minimum combination of variables obtained from the particle swarm. The procedure includes some constraints to force the optimization tool with the aim of determining the optimal values for the variables, minimizing the budget cost and, at the same time, complying with the solar fraction target. The Solar fraction (SF), evaluated as reported in Eq. 1, represents the percentage of electric energy required by the cooling plant that is covered by the solar field coupled with the electric energy storage. The residual fraction of energy is assumed to be provided by the national grid.

More precisely, the algorithm selects the best combination to achieve an annual solar fraction of 70% at the minimum budget cost. The objective function, listed in Eq. (2), represents the costs of the systems and includes a penalty function that rejects the solution that do not achieve the minimum solar fraction.

The optimization process is resumed in Fig. 9. The computer code simulates the building just at the first attempt whilst, the optimization tool launches several Trnsys simulations and evaluates network operation and cooling plant performance each time-step for 1-year period. The achieved solar fraction coupled with budget cost are adopted to select the new set of variables.

The cost evaluation considers the variation between individual user and industrial-grade components costs. The cost of the chiller is provided by the manufacturers while the cost of the PV is reported in the open literature [46] and [47]. The EES cost for large applications is based on the market analysis provided by [21] and for user applications in the manufacturer availability. The cost of a district network and its subsystem was estimated based on a technical report [48] and published data [47,48,]. Table 7 lists budget cost of the components adopted in the procedure.

$$SF = \frac{E_{PV} - export}{E_{chiller}} = \frac{E_{chiller} - import}{E_{chiller}} \tag{1}$$

$$f_{min} = A_{PV} \cdot Cost_{PV} + Cap_{CC} \cdot Cost_{CC} + Cap_{battery} \cdot Cost_{battery} + Penalty_{(SF<0.70)} \tag{2}$$

The optimum solutions, selected based on the previously described restrictions, are shown in Fig. 10 in terms of solar field aperture area, storage sizing, and rated chiller capacity. The DC-based option exhibits significantly better results and the trend shows a substantial increase in component size by moving to technologies with lower efficiency in terms of design COP. The optimization process selects the heat pump capacity greater than the peak cooling load to compensate for the temperature derating.

A more detailed analysis could be conducted by considering the average COP resulting from the annual simulation presented below. The nominal power consumption of chillers (Fig. 11-left) highlights the different chiller sizing between industrial and domestic solution. Chiller rated consumption shows a consistent advantage for DC which requires only 35% of the electricity compared to the home cooling system. The design efficiency of the chiller is reflected in the cooling energy stored in the battery (corresponding to the cooling capacity produced when the chiller is powered only by the battery) shown in Fig.11-right which is higher for district cooling despite the lower battery capacity.

Similarly, Fig. 12-left shows the operation of full load cooling in case of PV lack. The lower battery capacity (60%) of the centralized district system ensures a higher cooling production. Furthermore, the centralized DC adopts half of the solar field area to drives the chiller with a greater ratio of installed capacity to chiller demand, as shown in Fig. 12-right (equivalent to the Solar Multiple for concentrated solar power plant).

5. Results

The optimum solutions have been simulated for one year of operation. As an example, Fig. 13 shows a 3-day simulation of the centralized solar district cooling operation in the second week of February and in the last week of July, which represents the worst operation condition due to the high cooling demand and low heat rejection capability. The

Table 7
Budget costs

		District Cooling	5 gen District	Home cooling
Cost Chiller	USD/kW	140	500	800
Cost network	USD/N	7000	4000	0
Cost HX	USD/N	3000	3000	0
Cost PV	USD/kW	800	1200	1200
Cost PV	USD/m^2	119.2	178.8	178.8
Cost Storage EES	USD/kWh	328	510	510

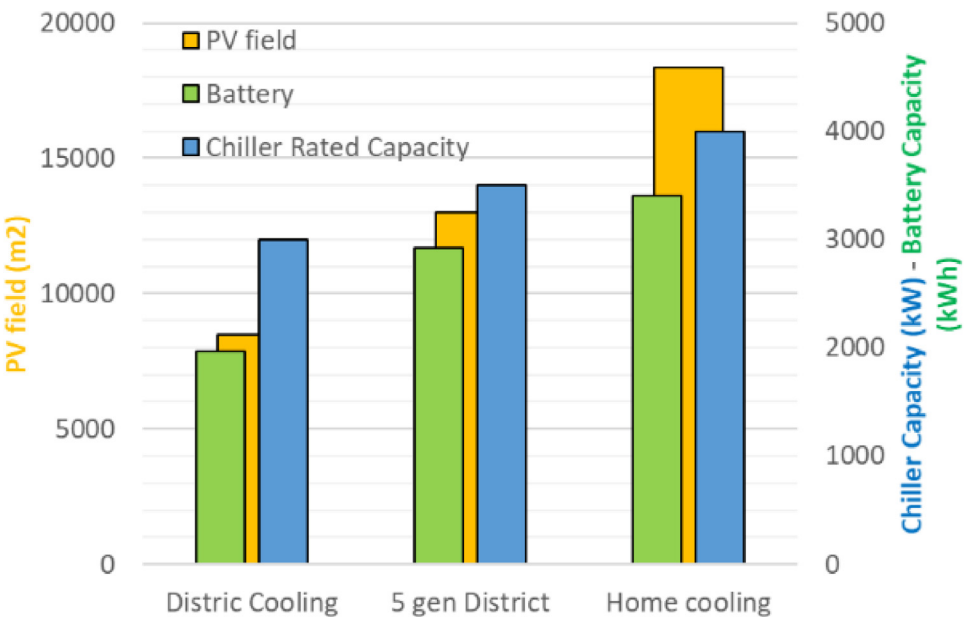

Fig. 10. Optimization result: components sizing

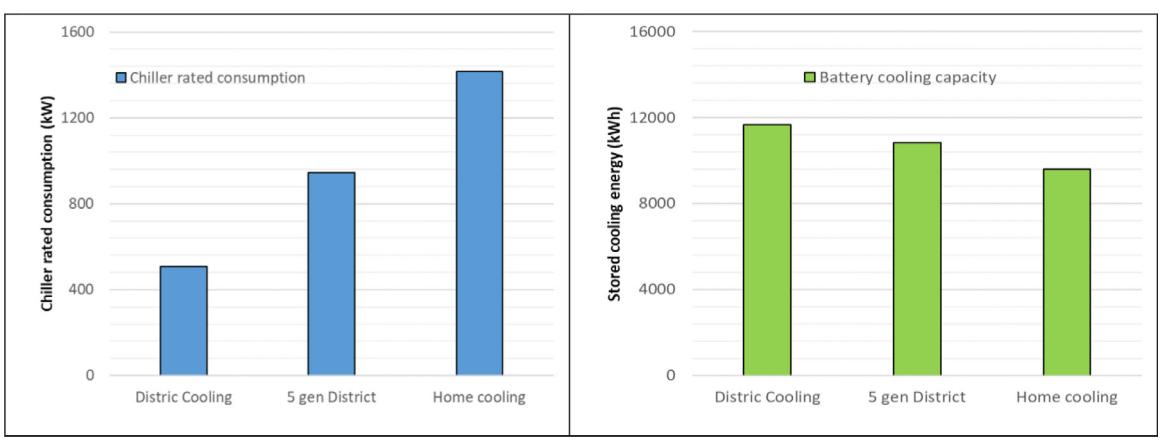

Fig. 11. Rated chiller consumption and cooling energy stored in the batteries

hourly trends of PV power generation, power import, and export, battery charge and discharge compared to the electric load emphasize the importance of transient analysis design process. The battery system allows to store part of the PV overproduction and largely supports the nighttime operation of the chiller. The load is fully met most of the time and the annual solar cooling achieved is equal to 70%.

The electricity consumption of the entire residential compound over one year is shown in Fig. 14 for the three system configurations in the form of hourly trend and duration curve. The solar district cooling network (light-blue line) and the 5th generation district system (yellow line) report limited fluctuations compared to the home air-cooled chiller (violet line); in the latter, in fact, the small size of the chiller unit and the significantly lower efficiency of the heat rejection system in hot climates have a detrimental impact on the annual energy consumption which reports an annual average COP of 2.83. A resume of the main parameters is listed in Table 8; the 5th-generation network shows an average annual COP of 3.701, while the centralized district cooling achieves a level of 5.92. As a result of the effects combination, COP vs chiller size and COP vs operating temperatures, the centralized district cooling requires half of the electric energy required by the home cooling to provide the same amount of chilled water to the users.

The following graphs, Figs. 15, 16 and 17, show the monthly energy balance for the three configurations analyzed. The results are divided as electric energy supplied to the system (PV self-consumption, energy from the battery, and import) and electric energy consumption/excess from the system (energy to the batteries, electric load, and export). The

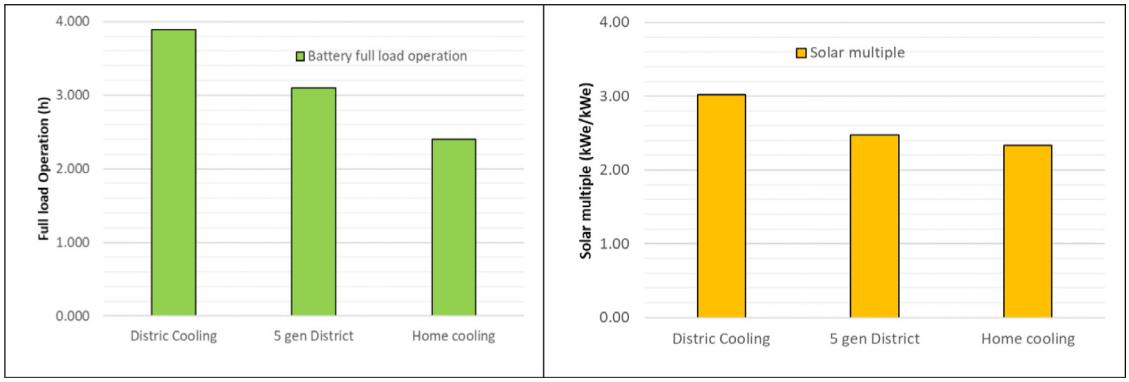

Fig. 12. Full load operation provided from the battery and solar multiple

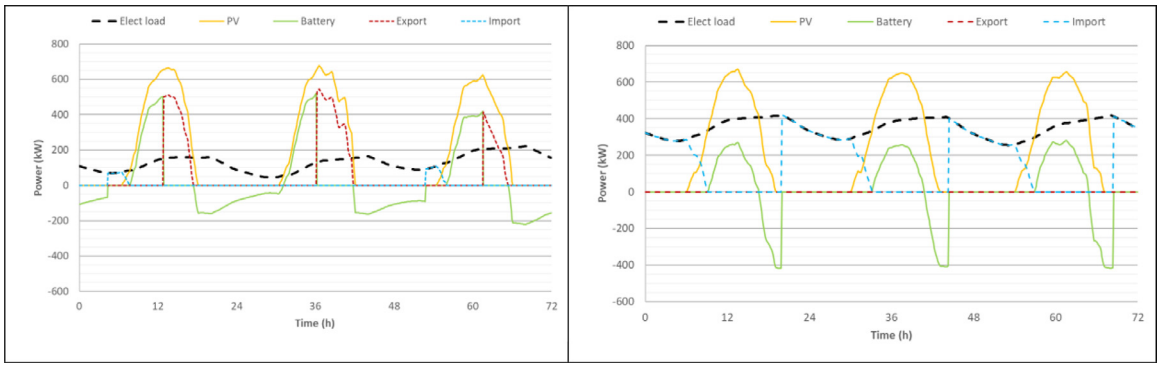

Fig. 13. Three days of detailed operation of centralized solar cooling (winter - summer)

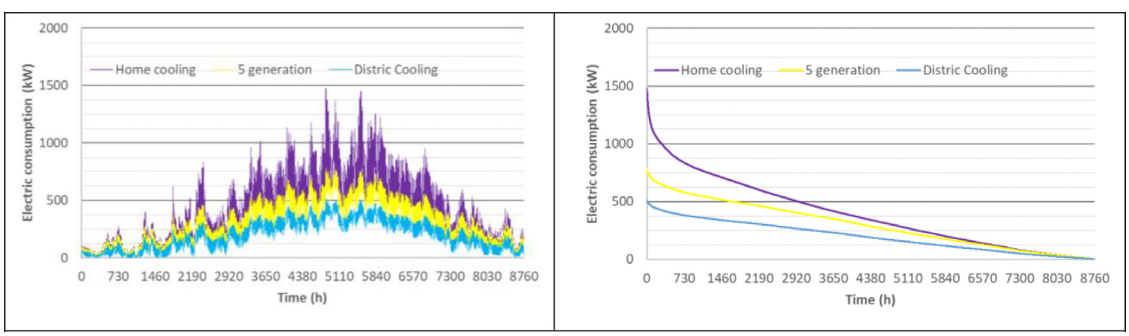

Fig. 14. Power consumption of the cooling plants

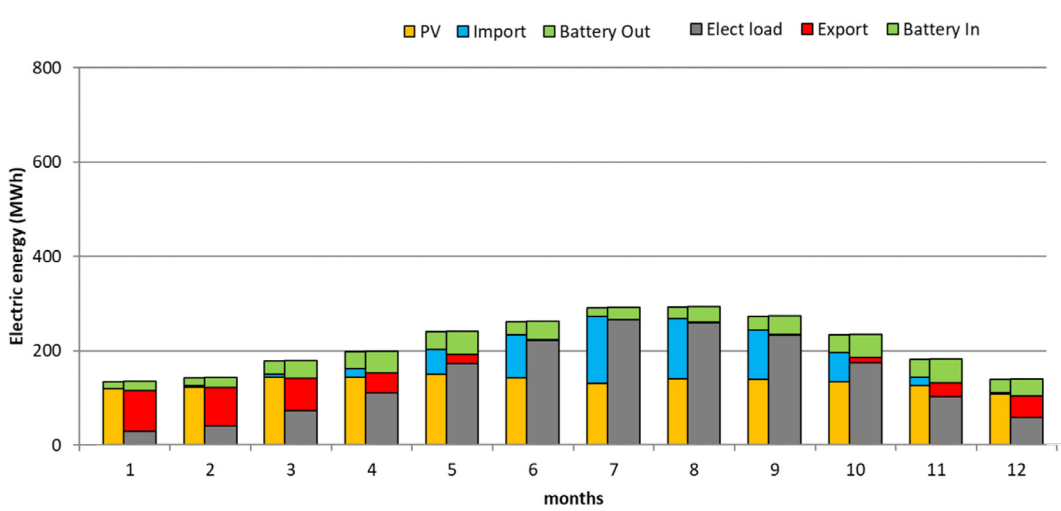

Fig. 15. Monthly integral values of power balance reported by the district cooling system

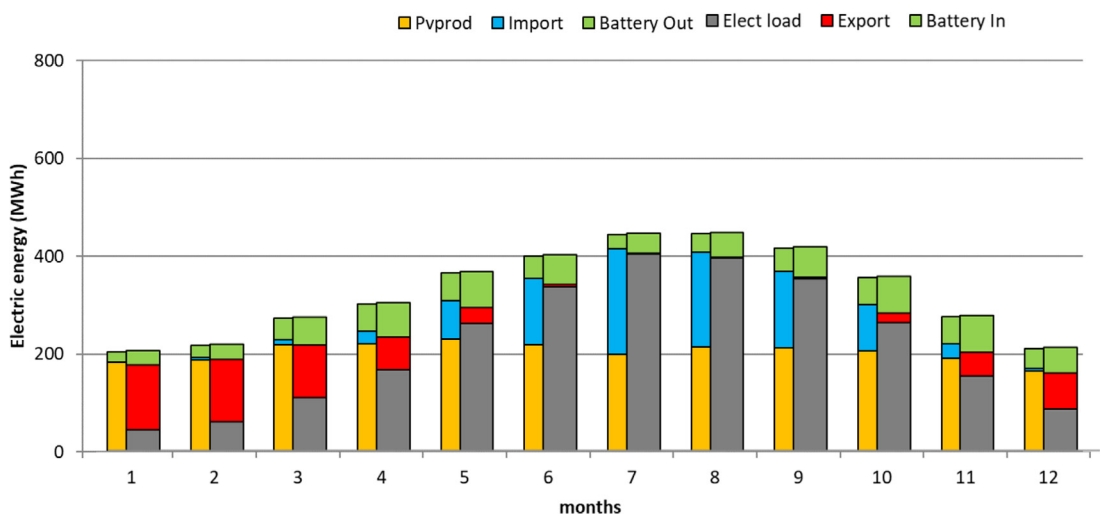

Fig. 16. Monthly integral values of power balance reported by the 5th gen district system

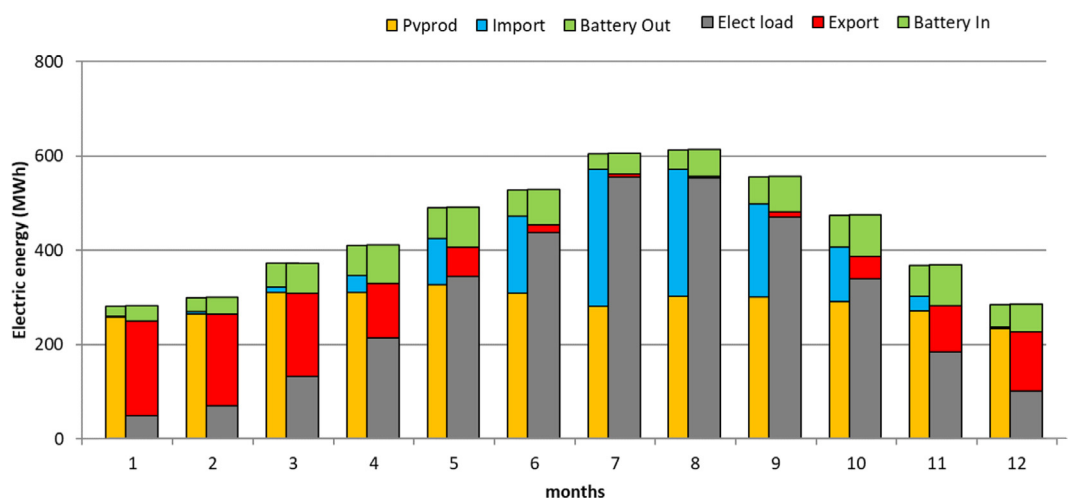

Fig. 17. Monthly integral values of power balance reported by the home cooling

Table 8
Energy balances of the optimum solutions

		District Cooling	5 gen District	Home cooling
Electric Load	kWh	1732211	2622345	3437407
PV production	kWh	1604034	2453228	3467543
from Battery	kWh	339944	512475	593358
Export	kWh	391210	617532	1061581
Import	kWh	628187	951560	1221199
COP (average)	-	5.917	3.705	2.827

PV field reports fairly constant production due to the high irradiation throughout the year, coupled with the summer high temperature and high humidity that affect the monthly production. Electric load trend forces the system to export most of the winter production while, in summer, import is required to balance the system. The electric energy storage covers the nighttime load in winter months and reduces energy fluctuation in summer when the load is higher. The trend is similar for the three plant layouts but with a large variation in terms of absolute energy values.

6. Economic considerations

Moving to the economic analysis, the evaluation considers the cost of all major components. The optimization presented in the previous paragraph ensures the best components sizing under the total budget cost minimization. The aim of the paragraph is to provide details about the cost allocation of the three different scenarios. The economic analysis does not include cost evaluation of a real business plan but considers costs that depend directly on the components size determined by the optimization algorithm.

The district system takes into account the network infrastructure, branches, heat exchangers, and metering systems according to published data [47,48]. Fig. 18a and Fig. 18b show the contribution of major components to the total primary cost in terms of absolute value and percentage. The impact of solar components on the cost is significant: the PV field and the energy storage represent more than 60% of the total CapEx for all cases but the left part of Fig. 18 shows the high cost difference between the systems. The cost of the chiller represents an increasing burden when moving from the centralized to the decentralized solution. The 5th generation district system suffers from cumulative cooling capacity (one single chiller for each building); in addition, the unidirectional en-

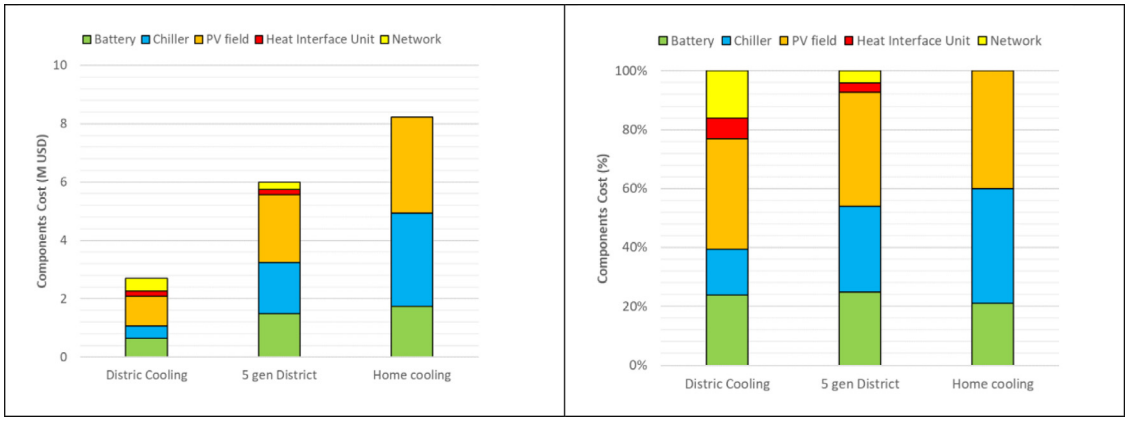

Fig. 18. Economic analysis of the optimum configurations

ergy flow (all users require only chilled water) makes balancing of the network ring very critical. The network components cost, as buried piping and user heat exchanger, is quite higher in a centralized system with respect to 5th generation system due to larger insulation required and the associated operation to realize the network branch. In both cases, the cost is compensated by the greater efficiency of the district-based systems with respect to the standard one.

To complete the assessment, the Levelized Cost of Cooling (LCOC) of the entire cooling production (renewable + standard) was calculated as listed in Eq. 3 according to a new approach as proposed in [49]. The LCOC was evaluated as the sum of the LCOCs of the individual components computed as reported in Eq. 4 (example referred to the PV system) including the operation and maintenance costs. The LCOC considers the balance between import and export of electric energy in a net-metering grid regulation with electricity cost equal to 0.05 USD/kWh. The CRF represents the Capital Recovery Factor evaluated as listed in Eq. 5, where Ny represents the component lifespan (50 years for network systems, 20 years for chillers, and 7 years for battery storage) and *i* represents the interest rate equal to 4%.

$$LCOC = LCOC_{PV} + LCOC_{EES} + LCOC_{DC} + LCOC_{CC} + \frac{E_{impot-export} \cdot E_{cost}}{Qcool} \quad (3)$$

$$LCOC_{PV}\ (USD/kWh) = \frac{CRF_{PV} \cdot C_{plant,PV}}{Qcool} + OM_{PV} \quad (4)$$

$$CRF_{PV} = \frac{i(1+i)^{Ny}}{(1+i)^{Ny} - 1} \quad (5)$$

The LCOC evaluation result shows a consistent reduction in the costs provided by district systems compared to the home system, more than what is reported by the installation costs. The LCOC results are 0.0277 USD/kWhc for the centralized district system compared with 0.0591 USD/kWhc for the 5th-generation district system and 0.0766 USD/kWhc for the home air conditioning system.

7. Conclusions

This paper presents a comparison of three different solar cooling systems: centralized district cooling system, 5th-generation district system and home AC system in the hot and humid climate of Abu Dhabi (UAE). The procedure includes modeling and evaluation of the cooling load of a residential neighborhood consisting of 62 single-family houses. A complex optimization procedure selects the minimum installation cost of the cooling systems under the constraint of an annual solar fraction of 70%. The performance of each solution was evaluated with a transient simulation under varying operating conditions for a period of 1 year. The optimal solution rewards the district systems-based option due to its better performance in consideration of solar resource utilization and operational efficiency compared to the standard solution that is affected by the variability of environmental conditions. Furthermore, the centralized district cooling shows an average annual COP of 5.92, while the 5th-generation network cannot guarantee a level higher than 3.701. From the economic point of view, the district systems propose a consistent reduction in terms of installation cost: - 65% for centralized district systems and -27% for 5th generation district systems.

References

[1] V. Eveloy, D.S. Ayou, Sustainable district cooling systems: status, challenges, and future opportunities, with emphasis on cooling-dominated regions, Energies 12 (2019), doi:10.3390/en12020235.
[2] A.A. Al-Ugla, M.A.I. El-Shaarawi, S.A.M. Said, Alternative designs for a 24-hours operating solar-powered LiBr - Water absorption air-conditioning technology, Int. J. Refrig. 53 (2015) 90–100, doi:10.1016/j.ijrefrig.2015.01.010.
[3] A. Mavrigiannaki, K. Gobakis, D. Kolokotsa, K. Kalaitzakis, A.L. Pisello, C. Piselli, et al., Zero energy concept at neighborhood level: a case study analysis, Solar Energy Adv. 1 (2021) 100002, doi:10.1016/j.seja.2021.100002.
[4] N. Perez-Mora, F. Bava, M. Andersen, C. Bales, G. Lennermo, C. Nielsen, et al., Solar district heating and cooling: a review, Int. J. Energy Res. 42 (2018) 1419–1441, doi:10.1002/er.3888.
[5] H. Lund, B. Möller, B.V. Mathiesen, A. Dyrelund, The role of district heating in future renewable energy systems, Energy 35 (2010) 1381–1390, doi:10.1016/j.energy.2009.11.023.
[6] L.A. Chidambaram, A.S. Ramana, G. Kamaraj, R. Velraj, Review of solar cooling methods and thermal storage options, Renew. Sustain. Energy Rev. 15 (2011) 3220–3228, doi:10.1016/j.rser.2011.04.018.
[7] M. Sameti, F. Haghighat, Optimization approaches in district heating and cooling thermal network, Energy Build. 140 (2017) 121–130, doi:10.1016/j.enbuild.2017.01.062.
[8] A.L.S. Chan, V.I. Hanby, T.T. Chow, Optimization of distribution piping network in district cooling system using genetic algorithm with local search, Energy Convers. Manage. 48 (2007) 2622–2629, doi:10.1016/j.enconman.2007.05.008.
[9] H. Lund, P.A. Østergaard, T.B. Nielsen, S. Werner, J.E. Thorsen, O. Gudmundsson, et al., Perspectives on fourth and fifth generation district heating, Energy 227 (2021) 120520, doi:10.1016/j.energy.2021.120520.
[10] S. Boesten, W. Ivens, S.C. Dekker, H. Eijdems, 5th generation district heating and cooling systems as a solution for renewable urban thermal energy supply, Adv. Geosci. 49 (2019) 129–136, doi:10.5194/adgeo-49-129-2019.
[11] M. Pellegrini, A. Bianchini, The innovative concept of cold district heating networks: a literature review, Energies 11 (2018) 236, doi:10.3390/en11010236.
[12] S. Buffa, M. Cozzini, M. D'Antoni, M. Baratieri, R Fedrizzi, 5th generation district heating and cooling systems: a review of existing cases in Europe, Renew. Sustain. Energy Rev. 104 (2019) 504–522, doi:10.1016/j.rser.2018.12.059.
[13] A. Arabkoohsar, M. Sadi, A solar PTC powered absorption chiller design for Co-supply of district heating and cooling systems in Denmark, Energy 193 (2020) 116789, doi:10.1016/j.energy.2019.116789.
[14] M. Sadi, A. Arabkoohsar, A.K. Joshi, Techno-economic optimization and improvement of combined solar-powered cooling system for storage of agricultural products, Sustain. Energy Technol. Assess. 45 (2021) 101057, doi:10.1016/j.seta.2021.101057.
[15] P. Denholm, R.M. Margolis, Evaluating the limits of solar photovoltaics (PV) in electric power systems utilizing energy storage and other enabling technologies, Energy Policy 35 (2007) 4424–4433, doi:10.1016/j.enpol.2007.03.004.
[16] K. Hara Chakravarty, M. Sadi, H. Chakravarty, A. Sulaiman Alsagri, T. James Howard, A Arabkoohsar, A review on integration of renewable energy processes

in vapor absorption chiller for sustainable cooling, Sustain. Energy Technol. Assess. 50 (2022) 101822, doi:10.1016/j.seta.2021.101822.
[17] A. Inayat, M. Raza, District cooling system via renewable energy sources: a review, Renew. Sustain. Energy Rev. 107 (2019) 360–373, doi:10.1016/j.rser.2019.03.023.
[18] L. Huang, R. Zheng, Energy and economic performance of solar cooling systems in the hot-summer and cold-winter zone, Buildings 8 (2018), doi:10.3390/buildings8030037.
[19] Prasanna A. Optimisation of a district energy system with a low temperature network 2017:17.
[20] C. Luerssen, H. Verbois, O. Gandhi, T. Reindl, C. Sekhar, D. Cheong, Global sensitivity and uncertainty analysis of the levelised cost of storage (LCOS) for solar-PV-powered cooling, Appl. Energy 286 (2021), doi:10.1016/j.apenergy.2021.116533.
[21] L. Goldie-Scot, A behind the scenes take on lithium-ion battery prices, BloombergNEF (2019) 1.
[22] Fu R., Remo T., Margolis R., Fu R., Remo T., Margolis R. 2018 U. S. utility-scale photovoltaics- plus-energy storage system costs benchmark. 2018.
[23] U. Eicker, D. Pietruschka, R. Pesch, Heat rejection and primary energy efficiency of solar driven absorption cooling systems, Int. J. Refrig. 35 (2012) 729–738, doi:10.1016/j.ijrefrig.2012.01.012.
[24] D.S. Kim, C.A Infante Ferreira, Air-cooled LiBr-water absorption chillers for solar air conditioning in extremely hot weathers, Energy Convers. Manage. 50 (2009) 1018–1025, doi:10.1016/j.enconman.2008.12.021.
[25] J. Muye, D.S. Ayou, R. Saravanan, A. Coronas, Performance study of a solar absorption power-cooling system, Appl. Therm. Eng. 97 (2016) 59–67, doi:10.1016/j.applthermaleng.2015.09.034.
[26] UN-ESCWA and BGR. Inventory of shared water resources in Western Asia - Umm er Radhuma- Dammam Aquifer System (Centre). Beirut: 2013.
[27] B. Morvaj, R. Evins, J. Carmeliet, Optimising urban energy systems: simultaneous system sizing, operation and district heating network layout, Energy 116 (2016) 619–636, doi:10.1016/j.energy.2016.09.139.
[28] H. Wang, W. Yin, E. Abdollahi, R. Lahdelma, W. Jiao, Modelling and optimization of CHP based district heating system with renewable energy production and energy storage, Appl. Energy 159 (2015) 401–421, doi:10.1016/j.apenergy.2015.09.020.
[29] T. Oppelt, T. Urbaneck, U. Gross, B. Platzer, Dynamic thermo-hydraulic model of district cooling networks, Appl. Therm. Eng. 102 (2016) 336–345, doi:10.1016/j.applthermaleng.2016.03.168.
[30] J. Zeng, J. Han, G. Zhang, Diameter optimization of district heating and cooling piping network based on hourly load, Appl. Therm. Eng. 107 (2016) 750–757, doi:10.1016/j.applthermaleng.2016.07.037.
[31] B. van der Heijde, M. Fuchs, C. Ribas Tugores, G. Schweiger, K. Sartor, D. Basciotti, et al., Dynamic equation-based thermo-hydraulic pipe model for district heating and cooling systems, Energy Convers. Manage. 151 (2017) 158–169, doi:10.1016/j.enconman.2017.08.072.
[32] H. Wang, H. Wang, H. Zhou, T. Zhu, Modeling and optimization for hydraulic performance design in multi-source district heating with fluctuating renewables, Energy Convers. Manage. 156 (2018) 113–129, doi:10.1016/j.enconman.2017.10.078.
[33] U. Eicker, D. Pietruschka, M. Haag, A. Schmitt, Energy and economic performance of solar cooling systems world wide, Energy Proc. 57 (2014) 2581–2589, doi:10.1016/j.egypro.2014.10.269.
[34] G. Franchini, G. Brumana, A. Perdichizzi, Performance prediction of a solar district cooling system in Riyadh, Saudi Arabia – a case study, Energy Convers. Manage. 166 (2018) 372–384, doi:10.1016/j.enconman.2018.04.048.
[35] G. Brumana, G. Franchini, E. Ghirardi, Optimization and performance assessment of a solar district cooling system, in: AIP Conference Proceedings, 2019 vol. 2191, doi:10.1063/1.5138759.
[36] J. Remund, S. Müller, S. Kunz, C. Schilter, Meteonorm Handbook part II: Theory, 2012.
[37] T.P. McDowell, D.E. Bradley, M. Hiller, J. Lam, J. Merk, W Keilholz, TRNSYS 18: the continued evolution of the software, Build. Simul. Conf. Proc. 4 (2017) 2049–2057, doi:10.26868/25222708.2017.516.
[38] M.C. Murray, N. Finlayson, M. Kummert, J. Macbeth, Live energy trnsys -trnsys simulation within google sketchup, IBPSA 2009 - Int. Build. Perform. Simul. Assoc. 2009 (2009) 1389–1396.
[39] Government of Dubai. Green building regulations & specifications. قفراشلا ةعماج 2012:1–75.
[40] G. Franchini, G. Brumana, A. Perdichizzi, Monitored performance of the first energy+ autonomous building in Dubai, Energy Build. 205 (2019) 109545, doi:10.1016/j.enbuild.2019.109545.
[41] R. Lund, S. Mohammadi, Choice of insulation standard for pipe networks in 4th generation district heating systems, Appl. Therm. Eng. 98 (2016) 256–264, doi:10.1016/j.applthermaleng.2015.12.015.
[42] H. Kristjansson, B. Bøhm, Advanced and traditional pipe systems: optimum design of distribution and service pipes, in: 10th International Symposium District Heating and Cooling, 2006, p. 11.
[43] ASHRAEFundamentals Handbook. S.I. Ameri, 1997.
[44] G. Brumana, G. Franchini, E. Ghirardi, A. Perdichizzi, Analysis of solar district cooling systems: the effect of heat rejection, E3S Web Conf. 197 (2020), doi:10.1051/e3sconf/202019708018.
[45] M. Wetter, GenOpt ® – A generic optimization program, in: Proc IBPSA's Building Simulation 2001 Conference, August 13-15, 2001 in Rio de Janeiro, 2001, p. 9.
[46] IRENA. Renewable power generation costs in 2018. 2018.
[47] R. Fu, D. Feldman, R. Margolis, U.S. solar photovoltaic system cost benchmark : Q1 2018, NREL (2018) 1–47, doi:10.7799/1325002.
[48] Davies G. The potential and costs of district heating networks 2009.
[49] G. Brumana, G. Franchini, E. Ghirardi, A. Perdichizzi, Techno-economic optimization of hybrid power generation systems: a renewables community case study, Energy 246 (2022) 123427, doi:10.1016/j.energy.2022.123427.